Article

Journal of
Nanoscience and Nanotechnology
Vol. 18, 7527–7531, 2018
www.aspbs.com/jnn

Effect of V-Pits on the Property of GaN Epilayer Grown by Metalorganic Chemical Vapor Deposition

Ying Hao Fu[1,2], Xiaojuan Sun[1,*], Jianwei Ben[1,2], Ke Jiang[1,2], Yuping Jia[1,*], Henan Liu[1], Zhiming Li[1], and Dabing Li[1]

[1] *State Key Laboratory of Luminescence and Applications, Changchun Institute of Optics, Fine Mechanics and Physics, Chinese Academy of Sciences, Changchun 130033, China*
[2] *University of Chinese Academy of Sciences, Beijing 101408, China*

Revealing the effect of the V-pits on the property of GaN is the key to understand and control the defects and thus to improve the performance in the GaN based devices. Here, the influence of the V-pits on the morphology, optics, structure and strain properties of GaN epilayer was investigated. The GaN films with different V-pits density were obtained by changing the growth parameters of metalorganic chemical vapor deposition. The scanning electron microscope, photoluminescence, high resolution X-ray diffraction and Raman were used to character the influence of V-pits on the GaN film. The results show that the sidewalls of V-pits might have higher bandgap than that of flat areas, which can suppress the shallow donor level related radiation recombination. Moreover, the V-pits can release the stress without apparently destroying the structural property. The results obtained here have importance of direction in controlling and taking advantage of V-pits.

Keywords: GaN, MOCVD, Defects, V-Pits.

1. INTRODUCTION

GaN is a promising material for optoelectronic and microelectronic devices such as light-emitting diodes, laser diodes, detectors, high electron mobility transistors due to its wide band gap and good thermal stability.[1–3] However, high density threading dislocations (TDs) exist in the GaN epilayer, which can act as nonradiative recombination sites, carrier scattering centers, current leakage paths, etc.[4,5] Thus, the electrical and optical performances including carrier mobility, leakage current, lifetime and quantum efficiency are dramatically deteriorated. Another common type of defects in GaN epilayer are hexagonal defects with pyramid shape also named V-defects or V-pits, the vertex of which have been found to originate from TDs.[6,7]

V-pits defects are widely investigated in InGaN/GaN multiple quantum wells (MQWs). It is well established that V-pits can open up to give nanotubes, which are associated with threading screw dislocations.[8] Transmission electron microscopy measurements also exhibited that some V-pits incorporated pure-edge dislocations.[9] So the TDs are considered to be the formation mechanism of V-pits where the $\{10\bar{1}1\}$ planes are stabilized. More investigations also gave the proof that V-pits may generate from the stacking mismatch boundaries induced by stacking faults or the 3D island coalescence.[10]

Differing from TDs, which may either prohibit light emission or increase the leakage and thus make the structures degrade quickly, the V-pits benefit the InGaN/GaN MQWs light emitting diodes (LEDs) by reducing the leakage and enhancing the efficiency. The V-pits show narrow sidewall quantum wells with an effective band gap larger than that of the regular *c*-plane quantum wells and thus form a potential landscape which effectively screens the defects themselves by providing an energy barrier around every defect.[11,12] But for the AlGaN based short-wavelength LEDs, the efficiency and lifetime are dramatically decreased when the TD density is larger than 1×10^8 cm^{-2}, even though V-pits also existed in the AlGaN based material.[13,14] So different effects of V-pits on the material properties are exhibited between the InGaN and AlGaN systems.

*Authors to whom correspondence should be addressed.

So far, whether the V-pits have the positive or negative effect on the GaN epilayer has not been studied in detail. In this paper, the effect of the V-pits on the properties of GaN epilayer grown by metalorganic chemical vapor deposition (MOCVD) was investigated. The results show that with the increase of the V-pits density, the full width at half maximum (FWHM) of photoluminescence (PL) of GaN film decreases, indicating that the V-pits can suppress the shallow donor level related radiation recombination. Moreover, the V-pits can release the stress without apparently destroying the structural property. The results presented here benefit us a lot to understand the V-pits in GaN based devices.

2. EXPERIMENTAL DETAILS

The unintentionally doped GaN epilayers with different V-pits densities were grown on 2 inch GaN/Sapphire template by MOCVD. Hydrogen (H_2) was used as carrier gas and trimethyl gallium (TMGa) and ammonia (NH_3) were used as Ga and N precursors, respectively. The GaN film was grown at 1050 °C with different TMGa and NH_3 flow rate. The thickness of GaN epilayers were about 2 μm for all the samples. Scanning electron microscope (SEM) measurement was employed to study the surface morphology. PL and high resolution X-ray diffraction (HRXRD) were used to determine the effect of V-pits on the optical and structural property. Raman measurements were utilized to analyze the relationship between the V-pits and the strain states. All the measurements were carried out at room temperature (RT).

3. RESULTS AND DISCUSSION

The SEM images of GaN epilayers grown by MOCVD with different V-pits density are shown in Figures 1(a) to (d). It shows that the density of V-pits increases gradually from Figures 1(a) to (d) by changing the growth parameters, named as sample 1 to 4, respectively. Some of the V-pits are larger than others in the samples. The larger size V-pits and smaller size V-pits may be formed on the screw dislocations and on the edge type dislocations, respectively.[15] The magnified SEM of the V-pits is shown in the insert of Figure 1(a). The dark spots are aligned to the V-pits center, considered to be the nanotubes associated with TDs. The densities of the V-pits from sample 1 to 4 are about 4.00×10^6 cm^{-2}, 1.75×10^7 cm^{-2}, 4.56×10^7 cm^{-2} and 8.00×10^7 cm^{-2}, respectively.

PL measurements were carried out to investigate the optical properties of samples with different V-pits density. Figure 2 shows the PL spectrum of samples 1 to 4. With the increase of V-pits, there are not obvious deep level radiation recombination related yellow luminescence peak located around 550 nm, which demonstrates that the V-pits may not introduce deep levels. The insertion is the enlarged spectrum of the peak area. As it can be seen

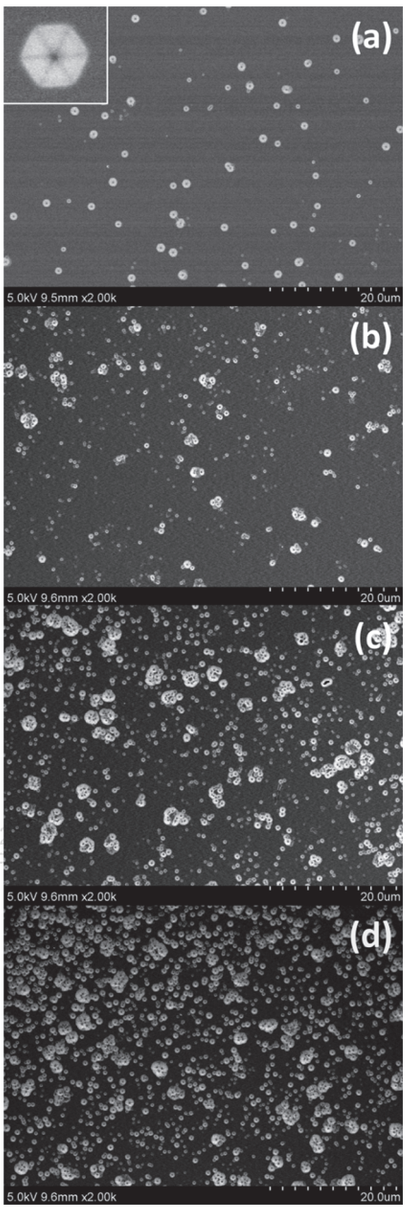

Figure 1. The SEM images of the morphology of GaN epilayers with different V-pit density. The insertion in (a) is the enlarged V-pit.

the peaks for all the four samples come from the band gap of GaN. For all samples there are shoulders at both sides of the PL peak. As mentioned above, the V-pits in InGaN/GaN MQWs have higher bandgap around the areas with V-pits than that without V-pits, which can suppress the carrier non-radiation recombination at the V-pits related TDs. Here, the very small shoulders at the short-wavelength side of the peaks indicate that there might also be bandgap increase around V-pits in GaN, similar to that in InGaN/GaN MQWs. As V-pits density increases, the relative intensity of short-wavelength shoulders to the main peaks increases since the higher V-pits density may

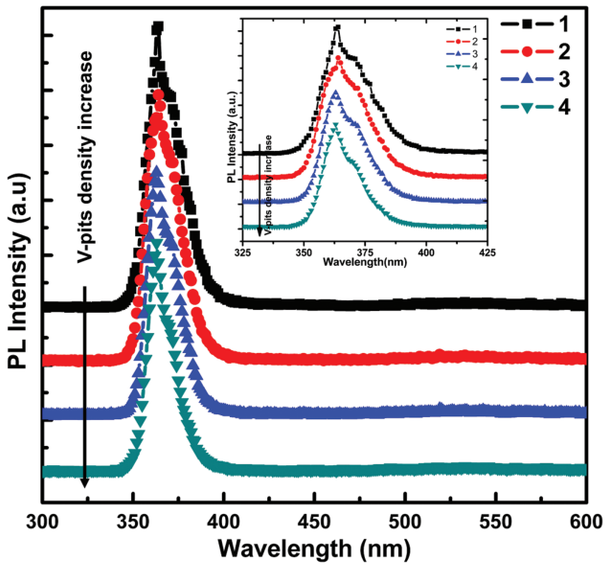

Figure 2. PL spectra of GaN epilayers with different V-pits density. The insertion is the enlarged spectrum of the peak area.

strengthen the sidewall effects. On the other hand, with the V-pits density increase, the relative intensity of the long-wavelength shoulders to the main peaks gradually decreases. Considering that the long-wavelength shoulders of the peaks are usually from the shallow donor energy levels, it can be deduced that the shallow donors may be suppressed by the V-pits.

To deeper understand the change of optical property with V-pits density, the integrated PL intensity, PL peak intensity, peak position and the FWHM were calculated, as shown in Figures 3(a) and (b). The integrated PL intensity means the total radiation recombination intensity for all kinds of mechanisms and the PL peak intensity reflects the band edge radiation recombination intensity. As V-pits density increases, both the integrated PL intensity and the peak intensity decrease, as shown in Figure 3(a). It can be explained that with the increase of V-pits density, the effective recombination area decreases, resulting in weaker PL intensity for all kinds of radiation recombination. Besides, the dependence of peak position and FWHM on V-pits density is displayed in Figure 3(b). For samples 1 and 2, the peak positions locate at 364 nm. For samples 3 and 4, the peak positions locate at 363 nm. This blue shift indicates that the samples with higher V-pits density have stronger sidewall effect. The FWHMs of the samples 1 to 4 are 20.8 nm, 20.9 nm, 19.0 nm and 16.4 nm, respectively. When the V-pits density is larger than 1.75×10^7 cm^{-2}, the FWHM reduces dramatically. These results demonstrate that the shallow donor level related radiation recombination mechanism is suppressed, which further proves that the bandgap of the sidewall areas is larger than the *c*-plane flat areas. It is correspondence with the phenomena exhibited in InGaN/GaN MQWs.

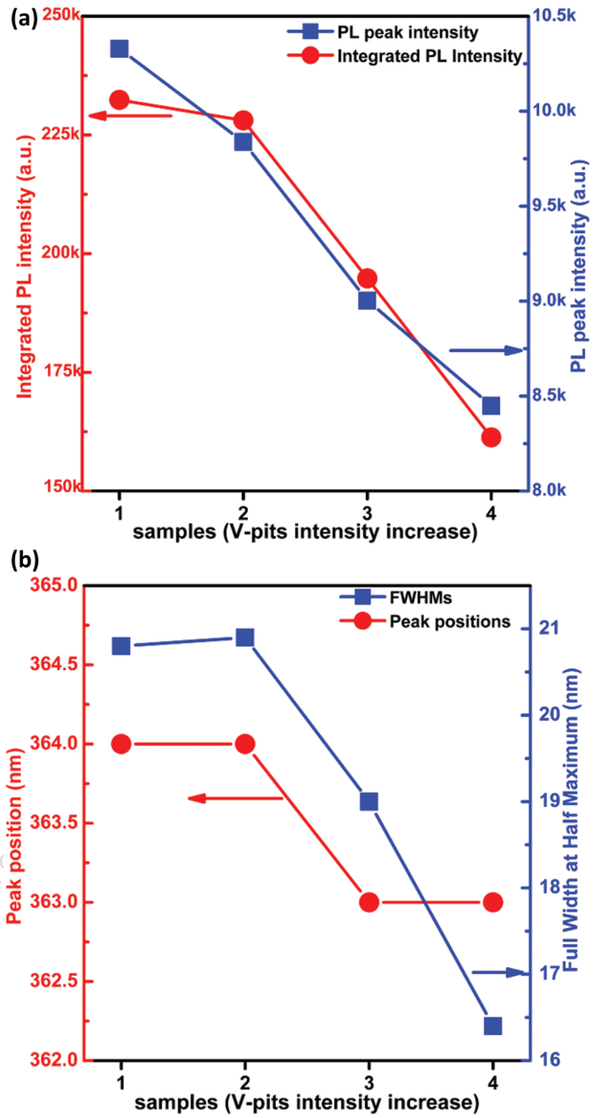

Figure 3. (a) The integrated PL intensities (left *Y* axis) and peak intensities (right *Y* axis) for samples 1 to 4. (b) The peak positions (left *Y* axis) and full width at half maximum (right *Y* axis) for samples 1 to 4.

To evaluate the effect of V-pits on the structural property of GaN epilayers, HRXRD is adopted here. The FWHM of (0002) plane XRD rocking curve (XRC) can reflect the density of screw dislocation while that of $(10\bar{1}2)$ plane can reflect the density of edge and mixed dislocation. The relationship between dislocation density and FWHM can be described as follows:[16]

$$\rho_s = \beta^2_{(0002)}/(2\pi \ln 2 \times |b_c|^2) \quad (1)$$

$$\rho_e = \beta^2_{(10\bar{1}2)}/(2\pi \ln 2 \times |b_a|^2) \quad (2)$$

in which β means the FWHM of XRC, $|b_c|$ and $|b_a|$ are the lengths of Burgers vector which equate to *c*-axial and *a*-axial lattice parameters, ρ_s means the density of screw

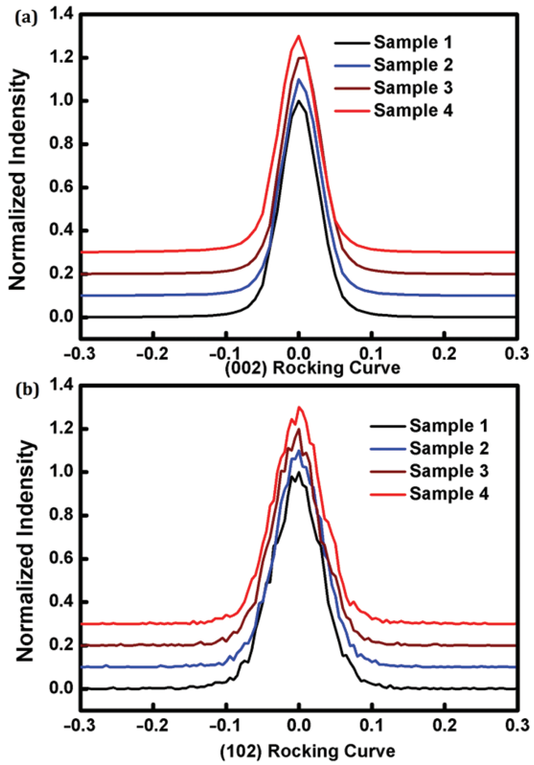

Figure 4. The (a) (0002) and (b) (10$\bar{1}$2) planes XRC results of samples 1 to 4.

dislocation and ρ_e stands for the density of edge and mixed dislocations, respectively.

Figure 4(a) shows the (0002) plane XRC results of the samples with different V-pits density. It can be found that even though the V-pits density increases from sample 1 to 4, the FWHM of the (0002) plane XRC keeps unchanged basically. Based on the Eq. (1), the screw dislocation was calculated, as shown in Table I. The V-pits densities of the four samples are also listed in Table I. The result shows that the screw dislocation density is higher than that of the V-pits density for all the samples. In addition, as the V-pits density increases, the screw dislocation does not show corresponding increase. The screw dislocation densities of samples 3 and 4 are even lower than those of samples 1 and 2. The (10$\bar{1}$2) plane XRC results of the four samples are shown in Figure 4(b). The densities of edge dislocation are calculated based on Eq. (2) and listed in Table I. Similar to the screw dislocation, the edge dislocation is not affected obviously by the V-pits, which indicates that the V-pits do not destroy the structural property though some of them may be generated from the dislocations.[6]

Table I. Density of dislocations and V-pits for different samples.

Samples	1	2	3	4
(0002) FWHM (arcsec)	216	216	208.8	212.4
Density of screw dislocation ($\times 10^7$ cm^{-2})	9.37	9.37	8.75	9.06
(10$\bar{1}$2) FWHM (arcsec)	252	244.8	259.2	262.8
Density of edge dislocation ($\times 10^8$ cm^{-2})	3.36	3.17	3.55	3.65
Density of V-pits ($\times 10^7$ cm^{-2})	0.4	1.75	4.56	7.5

The influence of V-pits on the strain state is obtained from the Raman measurement. The atom vibration modes of E_1 (TO) and E_2 (high) are shown in Figure 5(a).[19] The shift of E_1 (TO) and E_2 (high) peak corresponds to the change of atomic oscillation in c plane. It has been reported that the residual stress will lead to the change of lattice constant in c plane as well as the mode frequency

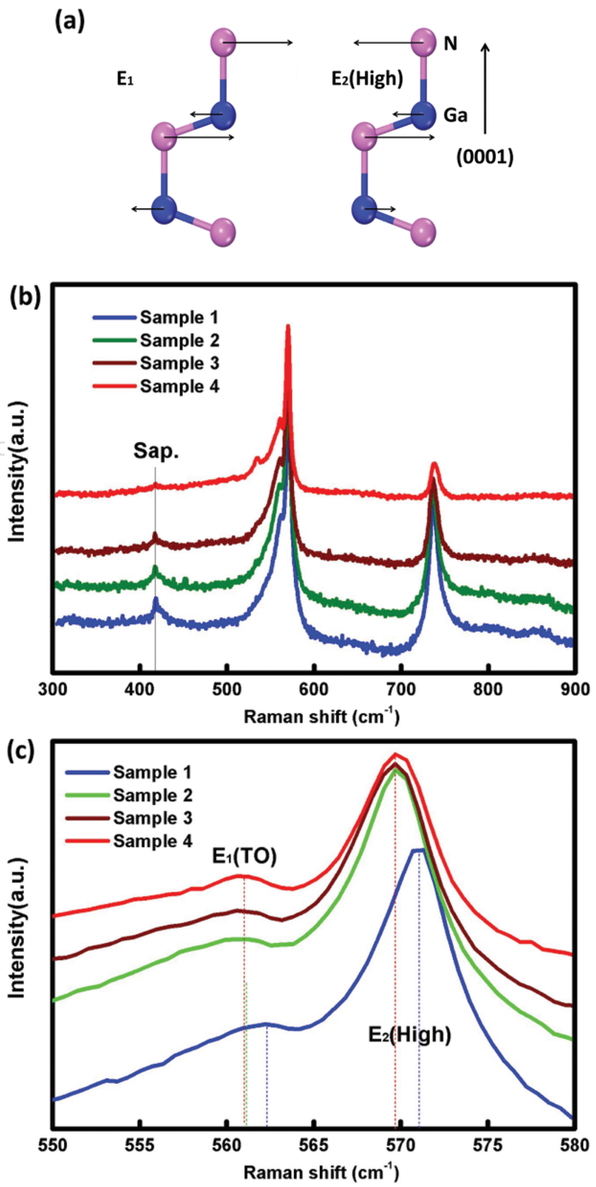

Figure 5. (a) Atom vibration modes of E_1 (TO) and E_2 (high) in hexagonal GaN. (b) Raman spectrum of different GaN samples. (c) The enlarged Raman spectrum of the E_2 (high) peak area.

of E_1 (TO) and E_2 (high) mode, so Raman test can measure the stress in GaN epilayer. The Raman spectrum of GaN epilayers with different V-pits density are shown in Figure 5(b). The peak positions of E_1 (TO) and E_2 (high) mode for bulk GaN are located at about 560 cm^{-1} and 568 cm^{-1}, respectively.[17] Compared with the bulk GaN, the GaN epilayers with different V-pits showed blue shift since the phonon frequency increases when the biaxial compressive stress increases, as shown in Figure 5(a). However, with the increase of the V-pits, the peak positions of samples 2 to 4 exhibit red shift compared to sample 1. Moreover, the peak of sample 4 with densest V-pits is close to that of the bulk GaN, indicating the V-pits can reduce the compressive stress in the epitaxial GaN layer. Furthermore, the E_1 (TO) mode appear and become stronger from samples 1 to 4 with the increase of V-pits density. According to the selection rule, the E_1 (TO) mode should be forbidden when the direction of Raman laser is parallel to c-axes.[18] The appearance and enhancement of the E_1 (TO) mode may result from the V-pits since they have an obliquity with c-axes. The more the V-pits density is, the higher the intensity of the E_1 (TO).

4. CONCLUSION

The effect of V-pits on the property of GaN epilayers was investigated. The samples with different V-pits density were prepared by MOCVD, about 4.00×10^6 cm^{-2}, 1.75×10^7 cm^{-2}, 4.56×10^7 cm^{-2}, 8×10^7 cm^{-2}, respectively. The SEM, PL, HRXRD and Raman measurement were used to reveal the relationship between the V-pits and the morphology, optics, structure and stain property. The results showed that with the increased density of V-pits, the shallow donor level related radiation recombination was suppressed because the sidewalls of V-pits might have higher bandgap than that of flat areas. In addition, the V-pits could release the stress in GaN epilayer while did not increase the screw and edge dislocation density.

Acknowledgments: This work was supported by the National Key R&D Program of China (2016YFB0400900), National Science Fund for Distinguished Young Scholars (61725403), the National Natural Science Foundation of China (61574142, 61322406, 61704171, 11705206), the Key Program of the International Partnership Program of CAS (181722KYSB20160015), the Special Project for Intergovernment Collaboration of the State Key Research and Development Program (2016YFE0118400), the Science and Technology Service Network Initiative of the Chinese Academy of Sciences, the Jilin Provincial Science and Technology Department (20150519001JH, 20180201026GX), the CAS Interdisciplinary Innovation Team, and the Youth Innovation Promotion Association of CAS (2015171).

References and Notes

1. D. B. Li, K. Jiang, X. J. Sun, and C. L. Guo, *Advances in Optics and Photonics* 10, 43 (**2018**).
2. S. H. Lim, Y. H. Ko, C. Rodriguez, S. H. Gong, and Y. H. Cho, *Light: Science and Applications* 5, e16030 (**2016**).
3. N. Sharma, C. Periasamy, and N. Chaturvedi, *J. Nanosci. Nanotechnol.* 18, 4580 (**2018**).
4. D. B. Li, X. J. Sun, H. Song, Z. M. Li, Y. R. Chen, G. Q. Miao, and H. Jiang, *Appl. Phys. Lett.* 98, 011108 (**2011**).
5. K. Ban, J. Yamamoto, K. Takeda, K. Ide, M. Iwaya, T. Takeuchi, S. Kamiyama, I. Akasaki, and H. Amano, *Applied Physics Express* 4, 052101 (**2011**).
6. K. S. Son, D. G. Kim, H. K. Cho, K. Lee, S. Kim, and K. Park, *Journal of Crystal Growth* 261, 50 (**2004**).
7. M. Zhang, D. M. Cai, Y. M. Zhang, X. J. Su, T. F. Zhou, M. Cui, C. Li, J. F. Wang, and K. Xu, *Mater. Lett.* 198, 12 (**2017**).
8. Z. L. Weber, Y. Chen, S. Ruvimov, and J. Washburn, *Phys. Rev. Lett.* 79, 2835 (**1997**).
9. N. Sharma, P. Thomas, D. Tricker, and C. Humphreys, *Appl. Phys. Lett.* 77, 1274 (**2000**).
10. H. K. Cho, J. Y. Lee, and G. M. Yang, *Appl. Phys. Lett.* 80, 1370 (**2002**).
11. A. Hangleiter, F. Hitzel, C. Netzel, D. Fuhrmann, U. Rossow, G. Ade, and P. Hinze, *Phys. Rev. Lett.* 95, 127402 (**2005**).
12. M. K. Kim, S. Choi, J. H. Lee, C. H. Park, T. H. Chung, J. H. Baek, and Y. H. Cho, *Scientific Reports* 7, 42221 (**2017**).
13. M. Kneissl, T. Kolbe, C. Chua, V. Kueller, N. Lobo, J. Stellmach, A. Knauer, H. Rodriguez, S. Einfeldt, Z. Yang, N. M. Johnson, and M. Weyers, *Semiconductor Science and Technology* 26, 014036 (**2011**).
14. A. Khan, K. Balakrishnan, and T. Katona, *Nat. Photonics* 2, 77 (**2008**).
15. J. L. Weyher, *Superlattices Microstructure* 40, 279 (**2006**).
16. W. K. Luo, L. Li, Z. H. Li, X. Dong, D. Q. Peng, D. G. Zhang, and X. J. Xu, *J. Alloys Compd.* 633, 494 (**2015**).
17. P. Perlin, C. Jauberthie-Carillon, J. P. Itie, A. S. Miguel, I. Grzegory, and A. Polian, *Physical Review B* 45, 83 (**1992**).
18. H. Harima, *Journal of Physics: Condensed Matter* 14, R967 (**2002**).
19. F. C. Wang, C. L. Cheng, Y. F. Chen, C. F. Huang, and C. C. Yang, *Semiconductor Science and Technology* 22, 896 (**2007**).

Received: 12 January 2018. Accepted: 24 March 2018.